

## Strongly Enhanced Magnetic Excitations Near the Quantum Critical Point of $\text{Cr}_{1-x}\text{V}_x$ and Why Strong Exchange Enhancement Need Not Imply Heavy Fermion Behavior

S. M. Hayden,<sup>1</sup> R. Double,<sup>1</sup> G. Aeppli,<sup>2</sup> T. G. Perring,<sup>3</sup> and E. Fawcett<sup>4</sup>

<sup>1</sup>*H. H. Wills Physics Laboratory, University of Bristol, Tyndall Avenue, Bristol BS8 1TL, United Kingdom*

<sup>2</sup>*NEC Research Institute, 4 Independence Way, Princeton, New Jersey 08540*

<sup>3</sup>*ISIS Facility, Rutherford Appleton Laboratory, Chilton, Didcot OX11 0QX, United Kingdom*

<sup>4</sup>*Department of Physics, University of Toronto, Toronto, Canada M5S 1A7*

(Received 17 August 1999)

Inelastic neutron scattering reveals strong spin fluctuations with energies as high as 0.4 eV in the nearly antiferromagnetic metal  $\text{Cr}_{0.95}\text{V}_{0.05}$ . The magnetic response is well described by a modified Millis-Monien-Pines function. From the low-energy response, we deduce a large exchange enhancement, more than an order of magnitude larger than the corresponding enhancement of the low-temperature electronic heat capacity  $\gamma T$ . A scaling relationship between  $\gamma$  and the inverse of the wave vector-averaged spin relaxation rate  $\Gamma_{\text{ave}}$  is demonstrated for a number of magnetically correlated metals.

PACS numbers: 75.40.Gb, 61.12.-q, 75.20.En

Many metals close to a magnetic instability at low temperatures display novel behavior in their physical properties, for example, a linear temperature dependence of the resistivity. Notable examples include the lamellar CuO systems [1], non-Fermi liquid systems [2], heavy fermions [3], and nearly ferromagnetic metals [4]. The proximity of an antiferromagnetic phase is also widely believed to be related to the occurrence of some forms of superconductivity [5]. Clearly, the magnetic excitations are largely responsible for the properties of such materials. In this paper, we study the magnetic excitations near the quantum critical point (QCP) of the structurally simple (body centered cubic)  $3d$  metal  $\text{Cr}_{1-x}\text{V}_x$ . For  $x \leq 0.35$ ,  $\text{Cr}_{1-x}\text{V}_x$  displays antiferromagnetic order in the form of an incommensurate spin density wave as in pure chromium [6]. The point ( $x = 0.35, T = 0$ ) in the  $x$ - $T$  plane [see Fig. 1(a)] is a QCP where a phase transition (the ordering of  $3d$  moments) occurs at zero temperature.

We studied the nearly antiferromagnetic composition  $\text{Cr}_{0.95}\text{V}_{0.05}$ . Strong magnetic excitations were observed: in common with  $4f$  and  $5f$  materials near quantum criticality. However, the excitations in  $\text{Cr}_{0.95}\text{V}_{0.05}$  are strong only in a small portion of reciprocal space. Other findings of the present study are as follows: (i) magnetic excitations exist with energies comparable to those of the highest frequency spin waves in strong ferromagnets such as iron [7] and nickel [8]; (ii) a simple phenomenological response function with four parameters describes the magnetic response over an extremely wide (0.004–0.4 eV) energy range; (iii)  $\text{Cr}_{0.95}\text{V}_{0.05}$  shows a large exchange enhancement of  $28 \pm 4$ ; (iv) there is a universal relationship between the Brillouin zone (BZ) averaged spin relaxation rate and the electronic heat capacity for  $\text{Cr}_{0.95}\text{V}_{0.05}$  and other magnetically correlated metals; and (v) the low effective mass of the quasiparticles in  $\text{Cr}_{0.95}\text{V}_{0.05}$  which coexists with the high exchange enhancement is due to the small phase space occupied by the exchange enhanced fluctuations.

Reactor-based neutron scattering measurements have demonstrated the existence of incommensurate magnetic correlations in  $\text{Cr}_{0.95}\text{V}_{0.05}$  for thermal energies [9]. In particular, the low-frequency magnetic response peaks at six symmetry-equivalent positions near the H or (100)-type point of the BZ. By using the HET and MARI spectrometers [10] at the ISIS spallation source, we have extended the energy range by almost an order of magnitude. Absolute intensities were obtained via normalization to measured incoherent scattering from a vanadium standard and coherent phonon scattering from the sample [11]. The accuracy is about  $\pm 10\%$ . Our sample, from the Materials Preparation Center of Ames Laboratory, was a 47.9 g arc-melted single crystal. The lattice constant at  $T = 2$  K was  $a = 2.895$  Å. Elastic scans performed using a cold-source three-axis spectrometer ( $k_i = 1.5$  Å<sup>-1</sup>) revealed no antiferromagnetic order for temperatures as low as  $T = 2$  K.

Neutron scattering measures the imaginary part of the generalized magnetic susceptibility  $\chi''(\mathbf{Q}, \omega)$ , the cross section for a paramagnet such as  $\text{Cr}_{0.95}\text{V}_{0.05}$  is

$$\frac{d^2\sigma}{d\Omega dE} = (\gamma r_e)^2 \frac{k_f}{k_i} |F(\mathbf{Q})|^2 \left( \frac{2/\pi g^2 \mu_B^2}{1 - \exp(-\hbar\omega/kT)} \right) \times \chi''(\mathbf{Q}, \hbar\omega), \quad (1)$$

where  $(\gamma r_e)^2 = 0.2905$  b sr<sup>-1</sup>,  $\mathbf{k}_i$  and  $\mathbf{k}_f$  are the incident and final neutron wave vectors, and  $|F(\mathbf{Q})|^2$  is the magnetic form factor. We label wave vectors by their positions in reciprocal space  $\mathbf{Q} = (h, k, l)$ .

We first characterized the inelastic scattering at lower  $\omega$ . Previous measurements [9] have established that for  $\hbar\omega \approx 10$  meV, the magnetic response is peaked at the six equivalent positions  $\mathbf{Q}_\delta = (1 \pm \delta, 0, 0)$ ,  $(1, \pm \delta, 0)$ , and  $(1, 0, \pm \delta)$ . For an incident neutron energy  $E_i = 35$  meV, we probe the excitations in the  $(h, k, 0)$  plane near (100) for  $\hbar\omega \approx 25$  meV as shown in Fig. 1(b). Data collected

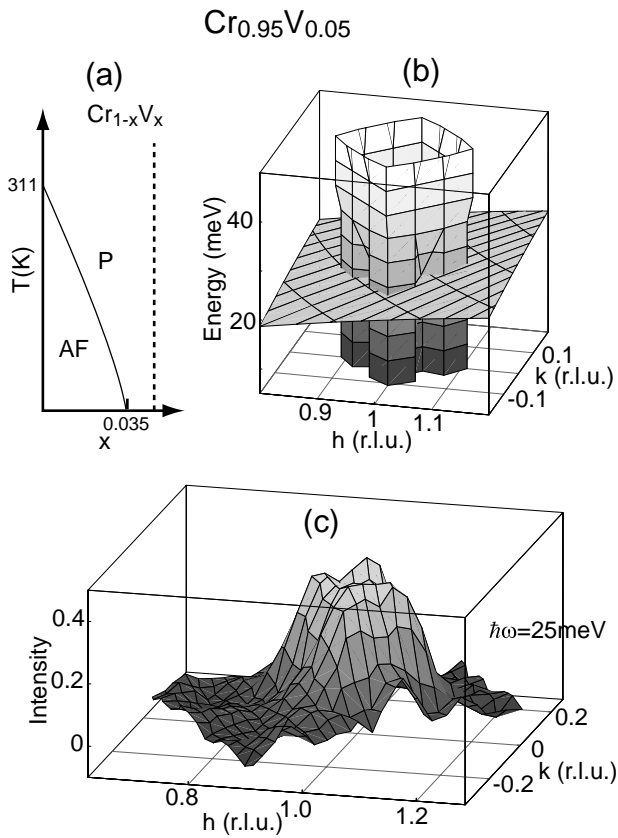


FIG. 1. (a) The magnetic phase diagram of the  $\text{Cr}_{1-x}\text{V}_x$  system showing the incommensurate antiferromagnet (AF) and paramagnetic (P) phases. The dotted line indicates the composition studied. (b) Schematic representation of the dynamic susceptibility  $\chi''(\mathbf{Q}, \omega)$  [Eq. (2)] of  $\text{Cr}_{0.95}\text{V}_{0.05}$  with experimentally determined parameters. For each energy, a contour at 1/2 the maximum value of  $\chi''(\mathbf{Q}, \omega)$  is drawn, the shading represents the maximum value. For  $E_i = 35$  meV,  $\chi''(\mathbf{Q}, \omega)$  is sampled on the grey surface. (c) Magnetic fluctuations near (100) in  $\text{Cr}_{0.95}\text{V}_{0.05}$  ( $T = 12$  K) measured using the HET spectrometer.

under these conditions are shown in Fig. 1(c). The response is a diffuse structure in  $\mathbf{Q}$  peaked near  $(1 \pm \delta, 0, 0)$  and  $(1, \pm \delta, 0)$ . One might visualize the overall magnetic response in  $\text{Cr}_{0.95}\text{V}_{0.05}$  as a “column” of scattering in  $\mathbf{Q} - \hbar\omega$  space as illustrated schematically in Fig. 1(b). By varying the incident energy  $E_i$ , we cut the column of scattering at different  $\omega$ . Figure 2 shows cuts along two perpendicular wave vector directions. At all  $\omega$  investigated, we observe a diffuse feature near the H position. The highest  $\omega$  investigated was  $\hbar\omega = 400$  meV, although the excitations probably exist up to even higher  $\omega$ . As the energy transfer increases the scattering broadens in wave vector and only one broad peak is observed at the highest  $\omega$  investigated. For all energies the response is significantly broader than the wave vector resolution.

A number of response functions have been used to describe nearly antiferromagnetic metals [12–17]. Following Zha *et al.* [16] for  $\text{La}_{2-x}\text{Sr}_x\text{CuO}_4$ , we use the function

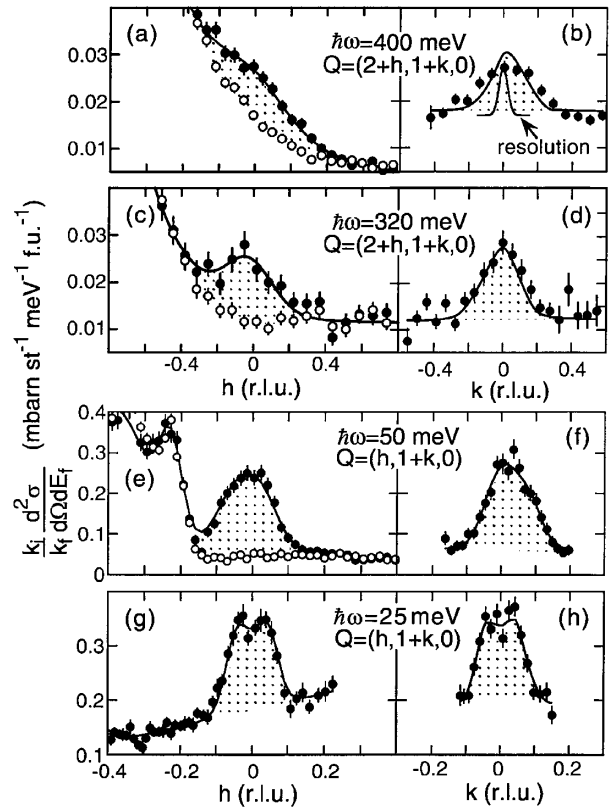


FIG. 2. Magnetic scattering near the (100) and (210) reciprocal space positions. By increasing the incident neutron energy, we are able to cut through the “column” of scattering depicted in Fig. 1(b) at different energy transfers. The left and right panels show cuts in two perpendicular reciprocal space directions. Open circles are a background measured at the same  $\omega$  and  $|\mathbf{Q}|$  but away from the H position, and the shaded area is the magnetic signal. The incident energies were (from bottom)  $E_i = 35, 110, 705, 860$  meV. Solid lines are resolution-corrected fits of Eq. (4) to the data.

$$\chi(\mathbf{Q}, \omega) = \sum_{\mathbf{Q}_\delta} \chi_\delta \left[ 1 + \frac{|\mathbf{Q} - \mathbf{Q}_\delta|^2}{\kappa_0^2} - i \frac{\omega}{\omega_{\text{SF}}} \right]^{-1}, \quad (2)$$

where the sum is over the six  $\mathbf{Q}_\delta$  positions surrounding the H point of the BZ. Equation (2) may be justified by expanding the Lindhard functions near the Fermi energy [12] and thus should describe a Fermi liquid. It also has a more general phenomenological justification in that it represents the first symmetry-allowed terms in a power series expansion of  $\chi^{-1}(\mathbf{Q}, \omega)$ . The observed scattering is related to the imaginary part of Eq. (2) which is

$$\chi''(\mathbf{Q}, \omega) = \sum_{\mathbf{Q}_\delta} \frac{\chi_\delta \kappa_0^4 [\omega / \omega_{\text{SF}}]}{[\kappa_0^2 + (\mathbf{Q} - \mathbf{Q}_\delta)^2]^2 + [\omega / \omega_{\text{SF}}]^2 \kappa_0^4}. \quad (3)$$

The physical meaning of the parameters in Eq. (2) is now clear.  $\chi_\delta$  determines the overall amplitude of the response. In the low-frequency limit  $\omega \ll \omega_{\text{SF}}$ , the position and sharpness of the peaks in wave vector are determined by

$\delta$  and  $\kappa_0$ , respectively. We find these parameters to be  $\delta = 0.08 \pm 0.01$  r.l.u. and  $\kappa_0 = 0.11 \pm 0.01 \text{ \AA}^{-1}$  from fitting low-frequency ( $\hbar\omega = 4$  meV) data collected on a cold-source triple axis spectrometer. Finally, the frequency dependence of the response, i.e., how the peak widths and amplitudes change with frequency, is controlled by the term  $(\omega/\omega_{\text{SF}})^2 \kappa_0^4$ , where  $\omega_{\text{SF}}$  is the characteristic frequency over which changes occur.

To test whether Eq. (3) describes the evolution of our data with  $\omega$ , we fitted cuts at each  $\omega$  using the general form

$$\chi''(\mathbf{Q}, \omega) = \sum_{\mathbf{Q}_\delta} \frac{\chi''_\delta(\omega) [\kappa_0^4 + \kappa_1^4(\omega)]}{[\kappa_0^2 + (\mathbf{Q} - \mathbf{Q}_\delta)^2]^2 + \kappa_1^4(\omega)}, \quad (4)$$

where the fitted  $\omega$ -dependent parameters  $\chi''_\delta(\omega)$  and  $\kappa_1(\omega)$  control the height and sharpness of the incommensurate peaks, respectively. The parameters  $\delta$  and  $\kappa_0$  were fixed at the values given above. If Eq. (3) describes the response, comparing Eqs. (3) and (4) predicts that the fitted parameters will vary as

$$\chi''_\delta(\omega) = \frac{\chi_\delta [\omega/\omega_{\text{SF}}]}{1 + [\omega^2/\omega_{\text{SF}}^2]} \quad (5)$$

and

$$\kappa_1^2(\omega) = \frac{\omega}{\omega_{\text{SF}}} \kappa_0^2. \quad (6)$$

The solid lines in Fig. 2 correspond to resolution-corrected fits of Eqs. (4)–(6) for different  $\omega$ . Figures 3(a) and 3(b) show the resulting  $\chi''_\delta(\omega)$  and  $\kappa_1^2(\omega)$  values for all data collected. The solid line in Fig. 3(a) is a fit of Eq. (5) which yields values for the spin fluctuation energy and amplitude parameters of  $\hbar\omega_{\text{SF}} = 88 \pm 10$  meV and  $\chi_\delta = (45 \pm 3) \mu_B^2 \text{ eV}^{-1} \text{ f.u.}^{-1}$ , respectively. Figure 3(b) shows that the width parameter  $\kappa_1^2$  displays an approximately linear variation with  $\omega$  as suggested by Eq. (6). The gradient of the fitted line  $\kappa_0^2/\omega_{\text{SF}} = 0.118 \pm 0.006 \text{ \AA}^{-2} \text{ eV}^{-1}$  gives a second estimate of  $\hbar\omega_{\text{SF}} = 102 \pm 24$  meV. Obtaining two indistinguishable estimates of  $\omega_{\text{SF}}$  in this way demonstrates that Eq. (2) provides a good description of our data: the  $\omega$  dependence of the amplitude and sharpness of the peaks are controlled by the parameter  $\omega_{\text{SF}}$ .

The starting point for models of the dynamic response of chromium and its alloys is the Fermi surface. It is believed that the peak in the dynamic susceptibility is due to the imperfect nesting of an electron “jack” and a larger hole “octahedron.” Staunton *et al.* [18] have recently performed *ab initio* calculations of the spin susceptibility for  $\text{Cr}_{0.95}\text{V}_{0.05}$ . To compare our results with these and other theoretical models, we have evaluated the  $\omega$  dependence of  $\chi''(\mathbf{Q}_\delta, \omega)$  for each  $\omega$  probed assuming Eq. (6). The resulting response is shown in Fig. 3(c).  $\chi''(\mathbf{Q}_\delta, \omega)$  differs from  $\chi''_\delta(\omega)$  because Eq. (3) sums contributions centered at six equivalent and nearby wave vectors  $\mathbf{Q}_\delta$ . The

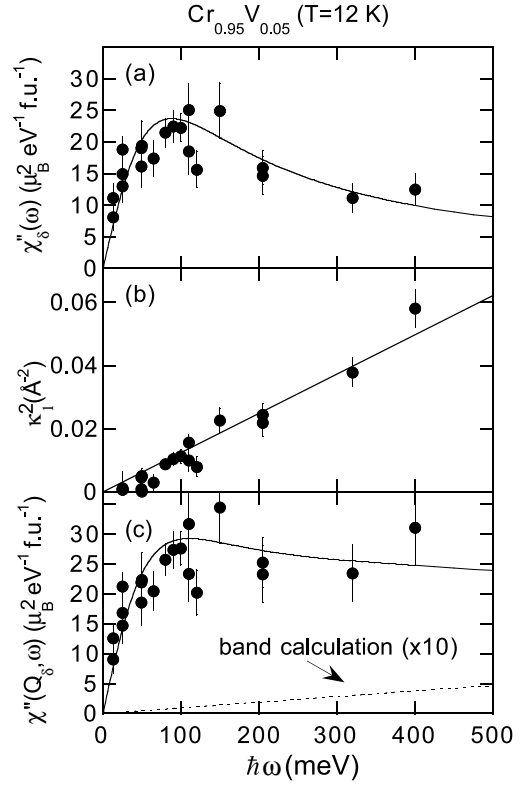


FIG. 3. The energy dependence of (a) the amplitude parameter  $\chi''_\delta(\omega)$ , (b) the sharpness parameter  $\kappa_1^2(\omega)$ , and (c) the susceptibility at the  $\mathbf{Q}_\delta$  position  $\chi''(\mathbf{Q}_\delta, \omega)$ .

dashed line in Fig. 3(c) shows the noninteracting susceptibility  $\chi_0''(\mathbf{Q}, \omega)$  calculated from the band structure and neglecting the exchange interaction, i.e., the bare Lindhard function [18]. Within a simple RPA model, the interacting susceptibility  $\chi(\mathbf{Q}_\delta, \omega)$  is given by  $\chi^{-1}(\mathbf{Q}, \omega) = \chi_0^{-1}(\mathbf{Q}, \omega) - \lambda$ , where  $\lambda$  is the mean field parameter describing the Coulomb interaction. In the low  $\omega$  limit  $\chi''(\mathbf{Q}, \omega) \propto \omega$  and

$$\chi''(\mathbf{Q}, \omega) = \frac{\chi_0''(\mathbf{Q}, \omega)}{[1 - \lambda\chi_0'(\mathbf{Q}, \omega)]^2}. \quad (7)$$

Comparing the initial gradients of the two lines in Fig. 3(c), we estimate the exchange enhancement factor  $[1 - \lambda\chi_0'(\mathbf{Q}_\delta, 0)]^{-1} = 28 \pm 4$ , demonstrating that  $\text{Cr}_{0.95}\text{V}_{0.05}$  is indeed very strongly exchange enhanced.

Many systems displaying strong magnetic fluctuations show dramatically renormalized thermodynamic properties. For example, heavy fermions exhibit a very large electronic linear heat capacity at low temperature. In spite of its large exchange enhancement,  $\text{Cr}_{0.95}\text{V}_{0.05}$  has a relatively small electronic specific heat  $\gamma T$ ,  $\gamma = 2 \text{ mJ K}^{-2}$  [19]. To understand why the quasiparticles in  $\text{Cr}_{0.95}\text{V}_{0.05}$  are not heavier, we must estimate the magnetic contribution to  $\gamma$ . If the excitations can be described as a set of overdamped oscillators with wave vector–dependent relaxation

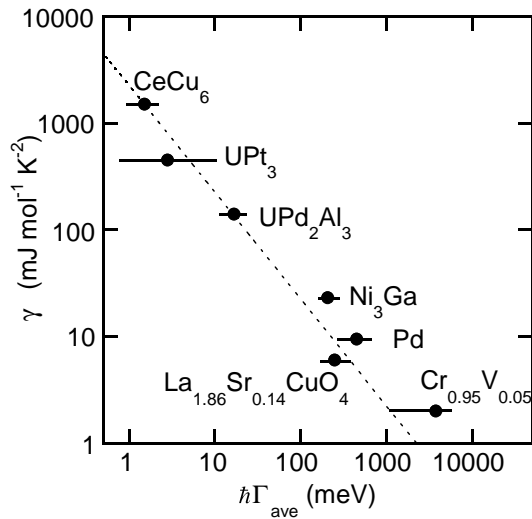


FIG. 4. The coefficient  $\gamma$  of the low-temperature electronic specific heat  $\gamma T$  is plotted against the wave vector-averaged spin relaxation rate  $\Gamma_{\text{ave}}$ , where  $\Gamma_{\text{ave}}^{-1} = \langle \Gamma^{-1}(\mathbf{Q}) \rangle_{\text{BZ}}$ .  $\Gamma_{\text{ave}}$  has been computed from data in Refs. [23], and horizontal bars are estimates of the uncertainty in  $\Gamma_{\text{ave}}$ . The dotted line is Eq. (8).

rate (characteristic frequency)  $\Gamma(\mathbf{Q})$ , then [20–22]

$$\gamma = \frac{\pi k_B^2}{\hbar} \frac{1}{\Gamma_{\text{ave}}} = \frac{\pi k_B^2}{\hbar} \left\langle \frac{1}{\Gamma(\mathbf{Q})} \right\rangle_{\text{BZ}}, \quad (8)$$

and  $\langle \rangle$  denotes a Brillouin-zone average. To put our results into a more general context, we have evaluated  $\Gamma_{\text{ave}}$  from Eq. (8) for  $\text{Cr}_{0.95}\text{V}_{0.05}$  and a number of other materials where the wave vector dependence of the magnetic response is known throughout a large part of reciprocal space. Figure 4 shows the results plotted against  $\gamma$ . The universal relationship Eq. (8) holds across widely differing systems such as 3d transition metals, their oxides, and heavy fermion compounds, demonstrating that the spin channel dominates the electronic entropy in all of these systems.

One might view the materials in Fig. 4 as being close to a QCP. Each of the materials has “soft” magnetic excitations in some region of reciprocal space. In spite of the large enhancement in  $\text{Cr}_{0.95}\text{V}_{0.05}$ , the magnetic fluctuations in a relatively small portion of reciprocal space (where  $\Gamma$  is small) contribute to  $\gamma$ . In contrast, the heavy fermion systems have large  $\gamma$  because the spin fluctuations are soft (have low  $\omega$ ) over larger portions of reciprocal space. For predominately antiferromagnetic fluctuations,  $\gamma$  scales roughly as  $\kappa_0^d/\omega_{\text{SF}}$ , where  $d$  is the system dimensionality. Thus, to raise  $\gamma$ , it is advantageous to lower  $d$  and  $\omega_{\text{SF}}$  and increase  $\kappa_0$ . Heavy fermion systems have larger  $\kappa_0$  and smaller  $\omega_{\text{SF}}$  than  $\text{Cr}_{0.95}\text{V}_{0.05}$  and hence larger  $\gamma$  values.

In summary, we have measured the high-frequency dynamic magnetic response of the paramagnetic alloy

$\text{Cr}_{0.95}\text{V}_{0.05}$  which is close to incommensurate magnetic order and has a large exchange enhancement. We observe strong magnetic correlations at epithermal energies up to 400 meV. The observed response can be described by a remarkably simple modified-MMP (Millis, Monien, and Pines) function where the  $\omega$  dependence of the response is controlled by a single parameter. We have computed the BZ average of the magnetic relaxation rate for  $\text{Cr}_{0.95}\text{V}_{0.05}$  and other materials close to magnetic order (or a QCP); this demonstrates the relationship between this quantity and the low-temperature quasiparticle specific heat, and also accounts for why  $\text{Cr}_{0.95}\text{V}_{0.05}$ , in spite of its large exchange enhancement, is not a heavy fermion system.

We are grateful for helpful discussions with P.W. Michell, J. Lowden, R. Fishman, J. Staunton, and O. Stockert.

- [1] M. A. Kastner *et al.*, Rev. Mod. Phys. **70**, 897 (1998).
- [2] *Proceedings of the Conference on Non-Fermi Liquid Behaviour in Metals, Santa Barbara, 1996* [J. Phys. C **8**, 9675–10 148 (1996)].
- [3] G. H. Lander and G. Aeppli, J. Magn. Magn. Mater. **100**, 151 (1991).
- [4] N. R. Bernhoeft *et al.*, Phys. Rev. Lett. **62**, 657 (1989).
- [5] N. D. Mathur *et al.*, Nature (London) **394**, 39 (1998).
- [6] E. Fawcett, Rev. Mod. Phys. **60**, 209 (1988), E. Fawcett *et al.*, *ibid.* **66**, 25 (1994).
- [7] D. McKenzie Paul *et al.*, Phys. Rev. B **38**, 580 (1988).
- [8] H. A. Mook and D. M. Paul, Phys. Rev. Lett. **54**, 227 (1985).
- [9] E. Fawcett *et al.*, Phys. Rev. Lett. **61**, 558 (1988); S. A. Werner *et al.*, J. Appl. Phys. **73**, 6454 (1993).
- [10] S. M. Hayden *et al.*, Physica (Amsterdam) **241–243B**, 241 (1998); **237**, 421 (1997).
- [11] R. Doubble, Ph.D. thesis, University of Bristol, 1998.
- [12] T. Moriya, Phys. Rev. Lett. **24**, 1433 (1970).
- [13] H. Sato and K. Maki, Int. J. Magn. **6**, 183 (1974).
- [14] A. J. Millis, H. Monien, and D. Pines, Phys. Rev. B **42**, 167 (1990).
- [15] D. R. Noakes *et al.*, Phys. Rev. Lett. **65**, 369 (1990).
- [16] Y. Zha, V. Barzykin, and D. Pines, Phys. Rev. B **54**, 7561 (1996).
- [17] G. Aeppli *et al.*, Science **278**, 1432 (1997).
- [18] J. B. Staunton *et al.*, Phys. Rev. Lett. **82**, 3340 (1999); (private communication).
- [19] F. Heiniger, Phys. Kondens. Mater. **5**, 285 (1966).
- [20] D. M. Edwards and G. G. Lonzarich, Philos. Mag. B **65**, 1185 (1992).
- [21] T. Moriya and T. Takimoto, J. Phys. Soc. Jpn. **64**, 960 (1995).
- [22]  $\Gamma$  is defined from the response of an overdamped oscillator  $\chi''(\mathbf{Q}, \omega) \propto \omega/(\omega^2 + \Gamma^2)$ .
- [23] L. P. Regnault *et al.*, J. Magn. Magn. Mater. **63–64**, 289 (1987) ( $\text{CeCu}_6$ ); Ref. [3] and N. R. Bernhoeft and G. G. Lonzarich, J. Phys. Condens. Matter **7**, 7325 (1995) ( $\text{UPt}_3$ ); N. R. Bernhoeft *et al.*, Phys. Rev. Lett. **81**, 4244 (1998) ( $\text{UPd}_2\text{Al}_3$ ); Ref. [4] ( $\text{Ni}_3\text{Ga}$ ); Ref. [11] ( $\text{Pd}$ ); Ref. [17] ( $\text{La}_{1-x}\text{Sr}_x\text{CuO}_4$ ).